PHYSICAL REVIEW E **98**, 010103(R) (2018)

Rapid Communications

Molecular dynamics determination of liquid-vapor coexistence in molten alkali halides

Maria C. Abramo,[1] Dino Costa,[1] Gianpietro Malescio,[1] Gianmarco Munaò,[2] Giuseppe Pellicane,[3]
Santi Prestipino,[1] and Carlo Caccamo[1,*]
[1]*Dipartimento di Scienze Matematiche e Informatiche, Scienze Fisiche e Scienze della Terra, Università degli Studi di Messina,*
Viale F. Stagno d'Alcontres 31, 98166 Messina, Italy
[2]*Dipartimento di Chimica e Biologia "Adolfo Zambelli," Università degli Studi di Salerno,*
via Giovanni Paolo II 132, 84084 Fisciano, Salerno, Italy
[3]*School of Chemistry and Physics, University of Kwazulu-Natal, Private Bag X01, Scottsville 3209, Pietermaritzburg, South Africa*

(Received 11 April 2018; published 19 July 2018)

We show by extensive molecular dynamics simulations that accurate predictions of liquid-vapor coexistence in molten alkali halides can be achieved in terms of a rigid ion potential description in which temperature-dependent ionic diameters are employed. The new ionic sizes result from the fitting of the experimental isothermal compressibilities, a condition whose physical implications and consequences are illustrated. The same diameters also allow us to formulate confident predictions for the compressibilities of salts in cases where the experimental data are lacking. The extension of the present approach to molten alkali-halide mixtures and to other classes of molten salts is discussed.

DOI: 10.1103/PhysRevE.98.010103

Molten salts of the alkali-halide family are an object of current interest since they form, under different configurations, the core environment of last-generation nuclear reactors [1–3]. They have also been intensively investigated in the past (see Refs. [4,5] and references therein), mainly for their possible use in nuclear reactors as heat exchangers. Molten alkali-halide mixtures are essential for the pyroprocessing of spent nuclear fuels (see Ref. [6] and references therein). In addition to this, different types of molten salts are currently employed for energy storage in solar thermodynamics plants (see Refs. [7,8] and references therein). With regard to all these systems, one important issue is the determination of their thermophysical properties (such as phase coexistence conditions, thermal expansivity, heat capacity, viscosity, and others), a knowledge that is severely hampered by the often very high temperatures involved. These experimental difficulties are a strong motivation for studies aimed to describe the phase behavior and other properties of molten salts by means of theoretical and computational approaches [9–13].

Historically, the microscopic description of molten alkali halides has been mostly based on the Born-Huggins-Mayer (BHM) analytic form of the interionic potential [14]

$$v_{ij}(r) = Z_i Z_j e^2/r + A\gamma_{ij}\exp[(\sigma_i+\sigma_j-r)/\lambda] - C_{ij}/r^6 - D_{ij}/r^8 \qquad (1)$$

with σ_i being the diameter of the ith ionic species as determined by Fumi and Tosi (FT) [14]. In Eq. (1) $Z_i = \pm 1$ is the ionic charge number, $A = 0.338 \times 10^{-17}$ J, the same for all alkali halides, $\gamma_{ij} = 1 + Z_i/n_i + Z_j/n_j$ with $n_i, n_j = 8$ except for $n_{Li^+} = 2$, λ is a parameter which varies from salt to salt, and C_{ij} and D_{ij} are van der Waals coefficients [14,15] (see also the Supplemental Material [16]). The BHM-FT interaction law was employed in computer simulation first for crystalline and then for molten alkali halides [4,5,17,18] with satisfactory results but also with some emerging limitations in the liquid state description (see Refs. [4,5,15] and references therein). In this respect, improvements over the rigid-ion BHM-FT model have been proposed, mainly in terms of polarizable ionic models and first-principle optimized model potentials (see Refs. [15,19,20] and references therein).

In this Rapid Communication, we report molecular dynamics (MD) simulations of molten alkali halides based on the BHM potential in which the ionic sizes are fixed so as to satisfy the condition

$$K_T^m = K_T^{exp}, \qquad (2)$$

where K_T^m and K_T^{exp} are the model and the experimental isothermal compressibility, respectively. A condition similar to Eq. (2) was employed some time ago in a work devoted to the determination of the structural properties of molten alkali halides [21]. In that case, the authors resorted to the well-known Weeks-Chandler-Andersen (WCA) theoretical [22–24] description of a short-range repulsive fluid of interest in terms of a hard-sphere reference fluid. Specifically, it was shown that by taking a charged hard-sphere (CHS) fluid as reference system, and provided the ionic fluid interactions are sufficiently steep at short range, a satisfactory approximation of the ionic fluid free energy to that of the CHS fluid is expressed by the condition (see Ref. [21] for details)

$$K_T^{CHS} = K_T^{exp}. \qquad (3)$$

K_T^{CHS} was then computed via an approximate theory [21] and equality (3) was enforced by means of an appropriate choice of the hard-sphere diameters.

In the present case, K_T^m will be computed via MD simulations of potential (1) with ionic sizes adjusted in such a way that

---

[*] Corresponding author: carlo.caccamo@unime.it

Eq. (2) is satisfied. However, since potential (1) is not hard-core repulsive at short range, it does not have the characteristics advocated by the WCA theory and owned by the CHS fluid; hence Eq. (2) cannot rigorously be obtained by applying that approach. In spite of this, a justification of condition (2) based on a WCA type of argument can be advanced. Indeed, we shall present below specific predictions for the BHM-FT potential clearly manifesting that the repulsive behavior of this model at small distances is significantly stronger than the actual ionic-fluid interactions, a circumstance signaling its higher proximity to the hard-core potential relative to the real system interactions. On the other hand, we will get indications that the enforcement of Eq. (2) leads to rather accurate predictions of liquid-vapor coexistence and of other thermodynamic quantities of molten alkali halides, thus providing an *a posteriori* justification for the use of that same condition.

We recall that in the BHM potential the FT ionic sizes σ_i [16], playing the role of repulsion parameters, were fixed through a fit of the ionic *crystal* free energies at *room* temperature [14]. Here, as a result of the fit of $K_\mathrm{T}^\mathrm{exp}$, performed over a temperature range extending from $\sim$1000 to $\sim$1300 K, the ionic sizes turn out to be rather regular decreasing functions of the temperature, well approximated by linear fitting laws. We then extend the applicability of such linear equations to very high temperatures, by thus determining ionic sizes up to the boiling point and also beyond, up to the critical temperature. As we shall illustrate, we assess the reliability of such an extrapolation by showing that the assumed diameters lead to quite an accurate determination of the overall liquid-vapor phase diagram of NaCl and KCl, and to similarly reliable predictions for the molar volumes of these two salts up to the respective boiling point temperatures. The pressures at the boiling point will also turn out qualitatively well predicted, as well as the critical temperatures and densities.

Our fitting procedure consists in constructing, for all molten salts, a small portion of a pressure isotherm at a temperature for which $K_\mathrm{T}^\mathrm{exp}$ of each salt is available [25]. To this aim we employ *NVT* molecular dynamics (MD) simulations with $N = 512$ total number of particles, increased in a few cases up to $N = 1024$ and 2048 in order to ascertain any size dependence of the simulation results [16]. The MD estimate of K_T^m is then obtained numerically from the isotherm slope [16] at the experimental density. In selected cases, the *NVT* estimates of K_T^m have been assessed by constant pressure *NPT* simulations in which the compressibility is computed from volume fluctuations. The two results always agree within 1–2% [16].

Several sets of isotherm calculations need to be implemented for each salt. We first use FT diameters: These systematically yield K_T^m lower than $K_\mathrm{T}^\mathrm{exp}$ (in agreement with early studies [4,5,17,18]) with an average underestimate of $\sim$25%. The BHM-FT model thus appears rather rigid and hence the potential is much steeper at short range than in real ionic fluid interactions, as previously anticipated. We then progressively reduce the FT ionic diameters in order to satisfy condition (2) while keeping, however, the FT crystal size ratio unaltered; we are thus assuming, as seems plausible to a first approximation, that the FT cation and anion diameters shrink in the same proportion [21]. Note that we are left, in this manner, with a *unique* adjustable parameter (the cation size, say) in the fit procedure. Usually several rescalings of the ionic size, and ensuing isotherm determination, are necessary before $K_\mathrm{T}^\mathrm{m} = K_\mathrm{T}^\mathrm{exp}$ within 1–2% or less.

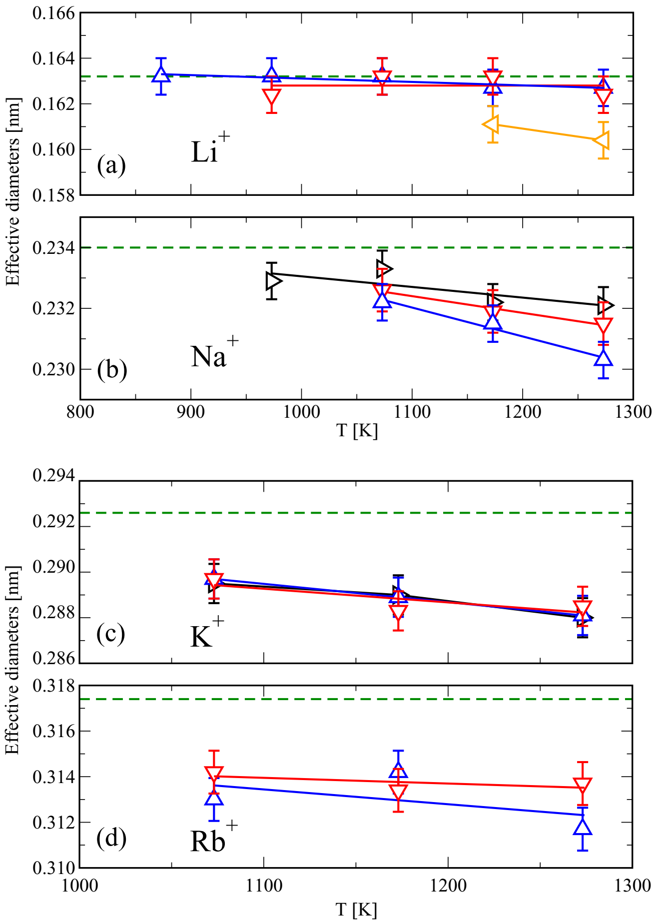

FIG. 1. Effective $K_\mathrm{T}^\mathrm{exp}$ fitting diameters as a function of the temperature. Triangles pointing left (orange), down (red), up (blue), and right (black), stand for cations (indicated in the panels) in fluoride, chloride, bromide, and iodide salts, respectively. Full lines are linear best fits to the displayed symbols, except for Li$^+$ in LiF (top panel). Note the use of a magnified vertical scale (fractions of 0.001 nm appreciable) to disentangle symbols, with some ensuing scattering of the points displayed. Note that Rb diameters are obtained by fitting K_T data not directly available from the experimental literature (see Ref. [16]). The dashed horizontal green line corresponds to the Fumi-Tosi crystal diameter of the cation in the panel. Error bars correspond to ±0.25% error on the diameter value estimate.

The above basic scheme is repeated for all T where $K_\mathrm{T}^\mathrm{exp}$ is available for the given salt [25], and replicated for each molten salt whenever the full set of potential (1) parameters *and* $K_\mathrm{T}^\mathrm{exp}$ are at disposal (conditions that are never jointly met for any of the Cs halides). The described sequence of calculations for all encompassed salts and temperatures has required about one 1000 simulation runs [16]. Results for the effective ionic sizes are displayed in Fig. 1. Numerical values are also reported in Ref. [16]. It immediately appears that the ionic sizes resulting from the above procedure turn out to be smaller, often by less than 1%, than their crystal values, and that they display an approximately linear decrease with increasing temperature.

This emerges from a linear regression analysis of the cation data: We find an average correlation coefficient $C \sim 0.85$,

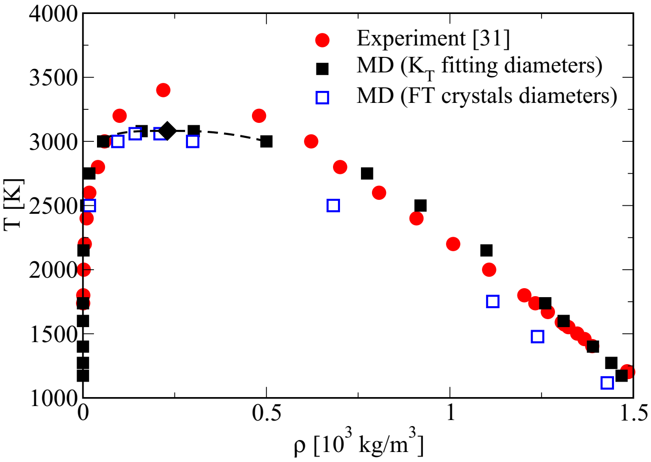

FIG. 2. Phase diagram of NaCl. Symbols as in the legend. The dashed line is the fit to the coexistence points through which our critical point (black diamond) is estimated (see text).

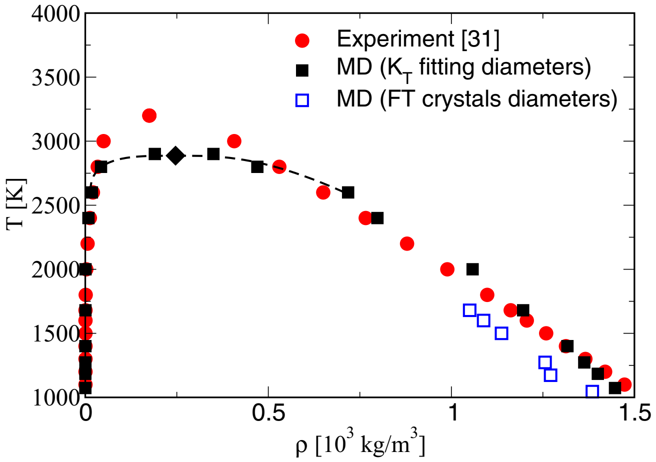

FIG. 3. Phase diagram of KCl. Graphic notations as in Fig. 2.

with several specific set showing $C = 0.985$, quite close to 1 (corresponding to fully linear behavior). Such linear fit lines are also displayed. It is worthwhile to mention, in this connection, that an even better defined linear dependence of the ionic diameters on T turns out in modified hypernetted chain theory [26–28] calculations that we have performed for the present BHM-FT model in which a similar fit $K_T^m = K_T^{exp}$ is imposed [16,29]. It also appears from Fig. 1 and from the numerical values of the diameters reported in Ref. [16] that cationic sizes at a fixed temperature show quite a moderate dependence on the specific salt, with variations of 0.0005 nm. The anion sizes are comparatively more sensitive: They show variation on the scale of 0.001–0.0015 nm (see Ref. [16]). The reason for this rests in our basic description scheme in which the compressibility fit essentially advocates a hard-sphere-like behavior of the BHM with respect to the real system, as discussed above. Clearly, such a representation is more realistic for the smaller cations than for the bigger anions, for which the definition of an effective "hard" size is less certain, as in fact it turns out.

We then employ the linear fit laws previously established to fix effective ionic sizes at very high temperatures. On such a basis, we can predict the liquid-vapor phase diagram of NaCl and KCl. The free energy and chemical potential necessary for the purpose have been computed by integrating the pressure with respect to the volume along isotherms at 1073, 1100, 1200, 1300, 1400, 1600, 1738, 2150, 2500, 2750, 3000, and 3080 K for NaCl and at 1073, 1184, 1273, 1680, 2000, 2400, 2600, 2800, 2900, and 3000 K for KCl. Fifty density values are explored in each case, more finely and with longer runs in the low-density region [16] (where sampling problems due to ionic association can take place; see Ref. [30]). The obtained phase diagram of NaCl is shown in Fig. 2.

We clearly see that the MD binodal points practically overlap to the experimental data [31] up to the boiling temperature (1738 K) at which we find liquid-vapor coexistence for a pressure of ~0 (10^5 Pa), in qualitative agreement with the expected experimental value of 10^5Pa (=1 bar).

As for the critical region, we assume scaling behavior with Ising exponents to hold very close to the critical point (see Ref. [32] and references therein); we thus fit coexistence points for $T \geqslant 3000$ K by assuming $(\rho_l - \rho_v) \propto (T - T_{cr})^\beta$ with $\beta = 0.323$, ρ_l and ρ_v being the liquid and vapor density at coexistence, respectively. We also make use of the law of rectilinear diameters. On such a basis we obtain the following estimates of the critical parameters: $T_{cr} = 3092$ K, $\rho_{cr} = 0.208 \times 10^3$ Kg/m^3. Our ρ_{cr} is fairly close to the experimental one of Ref. [31] (0.219×10^3 Kg/m^3) while our T_{cr} is somewhat lower than the corresponding estimate therein reported (3400 ± 200 K).

Then, we have constructed the $T - \rho$ binodal line of NaCl based on FT crystal diameters, closely reproducing the one reported by other authors in Ref. [30]: one finds in this case $T_{cr} = 3068$ K, $\rho_{cr} = 0.174 \times 10^3$ Kg/m^3. As visible in Fig. 2, this latter coexistence pattern comes out somehow less in density with respect to that based on rescaled diameters and to experiment. In the same Ref. [30] it is also shown that corresponding state arguments can lead to a definite improvement of the binodal line.

We have then attempted other linear fits of the Na diameters, different from the best fit shown in Fig. 1 (which has been used to calculate the coexistence data). We find that at 3000 K the ionic size can vary for at most 0.002 nm and that the effect on the estimated critical parameters is negligible.

The phase diagram of KCl is shown in Fig. 3. The MD binodal points well agree with the experimental data [31] up to the boiling temperature (1680 K), at which last T we find a coexistence pressure of ~0.6 (10^5 Pa), again in good qualitative agreement with experiment (10^5 Pa) [31]. We then find, through a procedure similar to that adopted for NaCl, the following critical parameters: $T_{cr} \sim 2886$ K against 3200 ± 200 K of the experiment [31] and $\rho_{cr} \sim 0.246 \times 10^3$ Kg/m^3, against $\rho_{cr} = 0.175 \pm 0.05 \times 10^3$ Kg/m^3 [31]. Predictions for liquid-vapor coexistence based on FT diameters are shown up to the boiling point temperatures. As found for NaCl, the liquid density is systematically underestimated by ~10% with respect to experiment.

We interpret the overall quite good assessment of liquid-vapor coexistence in both NaCl and KCl as an indication that the free energy of these molten salts is carefully predicted by the present application of potential (1). We surmise that this holds also for the other molten alkali halides.

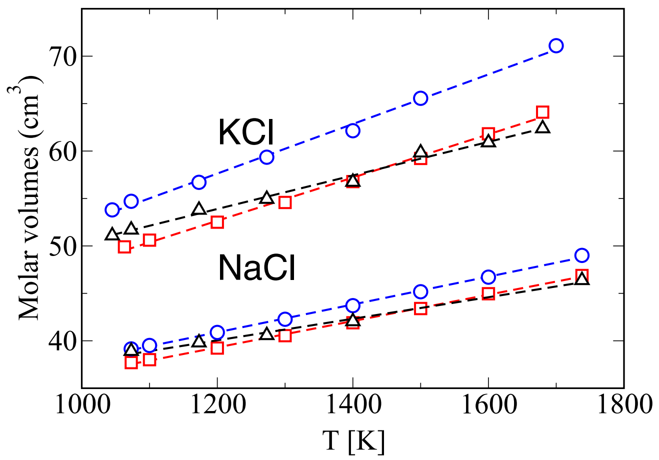

FIG. 4. Molar volumes obtained from temperature-dependent (triangles) and FT diameters (circles), as compared to experimental data [25] (squares). Errors on MD v_{M} are ~1% of the reported values. Dashed lines are best fit to MD and experimental data.

We have then determined the molar volumes $v_{\mathrm{M}}^{\mathrm{m}}$ of NaCl and KCl, from just above their melting temperature up to the respective boiling point; these two salts seem actually the only ones for which the experimental data $v_{\mathrm{M}}^{\mathrm{exp}}$ are available on such an extended temperature range. We do this by calculating, on the basis of $K_{\mathrm{T}}^{\mathrm{exp}}$ fitting diameters, $p-\rho$ isotherms encompassing the atmospheric pressure region. The $v_{\mathrm{M}}^{\mathrm{m}}$ thereby obtained are compared in Fig. 4 with those obtained through the FT crystal diameters, $v_{\mathrm{M}}^{\mathrm{FT}}$, and with experiment. As is clear, the estimates of $v_{\mathrm{M}}^{\mathrm{m}}$ are reasonably close to those of $v_{\mathrm{M}}^{\mathrm{exp}}$ whereas the values of $v_{\mathrm{M}}^{\mathrm{FT}}$ are significantly far away. Calculations of $v_{\mathrm{M}}^{\mathrm{m}}$ have also been performed in selected cases via *NPT* simulations. These reproduce quantitatively the *NVT* predictions.

Now, as already observed, $K_{\mathrm{T}}^{\mathrm{exp}}$ data are lacking for most molten alkali halides from ~1300 K up to the boiling temperature, and for some salts $K_{\mathrm{T}}^{\mathrm{exp}}$ is unknown even from above the melting temperatures to 1300 K. We then report some $K_{\mathrm{T}}^{\mathrm{m}}$ predictions in Fig. 5 for NaCl, KCl, and LiI, for which we hinge on the correspondence, previously established, between temperature-dependent diameters and fitted $K_{\mathrm{T}}^{\mathrm{exp}}$. In this connection, we note that the results for LiI could be obtained by taking advantage of the minor dependence of ionic diameters on the salt specificity so that, for instance, we could employ at 1073 K the iodine diameter of NaI at the same T [16]; the Li^+ diameter then follows from the $\mathrm{Li}^+/\mathrm{I}^-$ FT size ratio.

Further predictions of other thermodynamic quantities could be easily produced in this manner for several molten alkali halides. As for coexistence patterns, the experimental evidence is again restricted to quite a few molten alkali halides. We expect that the present approach should be able to provide at least qualitatively accurate results that can fill such a gap.

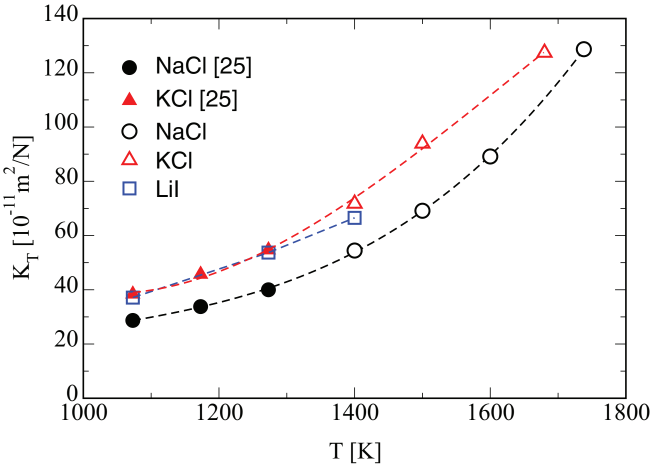

FIG. 5. K_{T} as a function of T. Full symbols, experiment [25]; open symbols, this work's predictions.

In conclusion, we would like to stress the more general applicability of our basic approximation scheme. Molten alkali-halide mixtures can, for instance, be soon investigated; this is of immediate interest since, e.g., molten NaCl-KCl mixtures are currently being considered for pyroprocessing of spent nuclear fuels [6], an important technological process which we have already alluded to. We have here shown how to generate liquid-vapor coexistence data for the pure salts involved; in order to deal with the mixture case, the change needed to the present approach would consist in the introduction of global density and concentration variables [33] in terms of which a condition similar to Eq. (2) (see previous discussions) should be rewritten. A compressibility fit condition could also be imposed in pairwise additive potential models of molten alkaline-earth-metal halides, or of other molten salts, should ionic size parameters be advocated for the description of short-range repulsive interactions and hence a rescaling of the ionic diameters similar to the one here employed be applicable. Phase coexistence calculations for all the systems just quoted are in program.

Of course, in relation to both present and future investigations, it must be remembered that the rigid-ion description here employed does not include either ionic polarizability or covalency effects, and these limitations could obviously affect its quantitative accuracy. It seems plausible, however, that in the very high temperature regime, i.e., significantly above the melting temperature, a major role should be played by basic interaction mechanisms as short-range steep repulsions and long-range Coulombic effects, and these are essentially included in the representation of potential (1). New evidence for salts and temperature ranges not hitherto explored would be then much needed at this stage for a further assessment of our rescaled size model.

[1] L. Mathieu *et al.*, Prog. Nucl. Energy **48**, 664 (2006).
[2] J. Serp *et al.*, Prog. Nucl. Energy **77**, 308 (2014).
[3] D. Heuer *et al.*, Ann. Nucl. Energy **64**, 421 (2014).
[4] J. Lewis, K. Singer, and L. Woodcock, J. Chem. Soc. Faraday Trans. II **71**, 301 (1975).
[5] J. W. E. Lewis and K. Singer, J. Chem. Soc. Faraday II **71**, 41 (1975).
[6] J. Song, S. Shi, X. Li, and L. Yan, J. Mol. Liq. **234**, 279 (2017).
[7] V. M. B. Nunes, C. S. Queiros, M. J. V. Lourenco, F. J. V. Santos, and C. A. Nieto de Castro, Appl. Energy **183**, 603 (2016).

[8] P. D. Myers and D. Y. Goswami, Appl. Therm. Eng. **109**, 889 (2016).
[9] J. L. Aragones, E. Sanz, C. Valeriani, and C. Vega, J. Chem. Phys. **137**, 104507 (2012).
[10] A. E. Gheribi *et al.*, Mol. Phys. **112**, 1306 (2014).
[11] V. Khokhlov, V. Ignatiev, and V. Afonichkin, J. Fluor. Chem. **130**, 30 (2009).
[12] M. Salanne, C. Simon, P. Turq, and P. A. Madden, J. Fluor. Chem. **130**, 38 (2009).
[13] L. C. Dewan, C. Simon, P. A. Madden, L. W. Hobbs, and M. Salanne, J. Nucl. Mat. **434**, 322 (2013).
[14] M. P. Tosi and F. Fumi, J. Phys. Chem. Solids **25**, 45 (1964).
[15] M. J. L. Sangster and M. Dixon, Adv. Phys. **25**, 247 (1976); M. Dixon and M. J. Gillan, Phil. Mag. B **43**, 1099 (1981).
[16] See Supplemental Material at http://link.aps.org/supplemental/10.1103/PhysRevE.98.010103 for additional information.
[17] L. V. Woodcock and K. Singer, Trans. Faraday Soc. **67**, 12 (1971).
[18] D. J. Adams, J. Chem. Soc. Faraday Trans. II **72**, 1372 (1976).
[19] M. Wilson and P. A. Madden, J. Phys. Condensed Matter **5**, 2687 (1993).
[20] P. A. Madden, R. Heaton, A. Aguado, and S. Jahn, J. Mol. Struct. TEOCHEM **771**, 9 (2006).
[21] M. C. Abramo, C. Caccamo, G. Pizzimenti, M. Parrinello, and M. P. Tosi, J. Chem. Phys. **68**, 2889 (1978).
[22] H. C. Andersen, J. D. Weeks, and D. Chandler, Phys. Rev A **4**, 1597 (1971); L. Verlet and J. J. Weis, Mol. Phys. **24**, 1013 (1972).
[23] L. L. Lee and D. Levesque, Mol. Phys. **26**, 1351 (1973).
[24] J.-P. Hansen and I. R. McDonald, *Theory of Simple Liquids* (Academic Press, London, 1976).
[25] G. J. Janz, *Molten Salts Handbook* (Academic Press, New York, 1967).
[26] Y. Rosenfeld and N. W. Ashcroft, Phys. Rev. A **20**, 1208 (1979).
[27] C. Caccamo, G. Malescio, and L. Reatto, J. Chem. Phys. **81**, 4093 (1984).
[28] C. Caccamo, Phys. Rep. **274**, 1 (1996).
[29] C. Caccamo (unpublished).
[30] Y. Guissani and B. Guillot, J. Chem. Phys. **101**, 490 (1994).
[31] A. D. Kirshenbaum, J. A. Cahill, P. J. McGonigal, and A. V. Grosse, J. Inorg. Nucl. Chem. **24**, 1287 (1962).
[32] Y. C. Kim, M. E. Fisher, and A. Z. Panagiotopoulos, Phys. Rev. Lett. **95**, 195703 (2005).
[33] N. H. March and M. P. Tosi, *Atomic Dynamics in Liquids* (Macmillan Press, London, 1976).